KaonLT BSA Analysis of p(e,e'π^+)n

Summary Tables

The following tables present the mean kinematics, final values of $\sigma_{LT'}/\sigma_0$ and its associated statistical and systematic uncertainties for each (Q^2,x_B) bin.

$\langle -t\rangle$ [GeV^2]	$-t$ range [GeV^2]	$\langle Q^2\rangle$ [GeV^2]	$\langle$W$\rangle$ [GeV]	$\langle x_B\rangle$	$\sigma_{LT'}/\sigma_0$	$\delta_{\rm stat}$	$\delta^{\downarrow}_{\rm sys}$	$\delta^{\uparrow}_{\rm sys}$
0.150	0.09 – 0.20	2.50	2.42	0.34	0.0852	0.0211	0.0054	0.0121
0.227	0.20 – 0.25	2.67	2.37	0.36	0.0764	0.0193	0.0075	0.0067
0.275	0.25 – 0.30	2.80	2.37	0.38	0.0570	0.0155	0.0028	0.0357
0.323	0.30 – 0.35	2.92	2.31	0.39	0.1133	0.0180	0.0057	0.0060
0.376	0.35 – 0.40	3.02	2.29	0.41	0.1263	0.0233	0.0115	0.0110
0.447	0.40 – 0.50	3.13	2.25	0.42	0.1259	0.0167	0.0071	0.0167
0.621	0.50 – 0.80	3.34	2.18	0.46	0.1479	0.0140	0.0138	0.0052

Table 1: Summary table for setting 1, at central values of Q^2=3.0 GeV^2, x_B=0.4, $\epsilon = 0.885$. The columns $\langle -t\rangle$, $\langle Q^2\rangle$, $\langle$W$\rangle$, and $\langle x_B\rangle$ denote the average value of the variable in the bin. The second column provides the borders of the bin. The columns $\delta_{\rm stat}$, $\delta^{\downarrow}_{\rm sys}$ and $\delta^{\uparrow}_{\rm sys}$ refer to the uncertainties of $\sigma_{LT'}/\sigma_0$. The systematic error is asymmetric, with $\delta^{\downarrow}_{\rm sys}$ ($\delta^{\uparrow}_{\rm sys}$) denoting the lower (upper) bounds. The total error in each direction is the sum of $\delta_{\rm stat}$ and $\delta^{\downarrow}_{\rm sys}$ ($\delta^{\uparrow}_{\rm sys}$) in quadrature. This table corresponds to Figure 5(a).

$\langle -t\rangle$ [GeV^2]	$-t$ range [GeV^2]	$\langle Q^2\rangle$ [GeV^2]	$\langle$W$\rangle$ [GeV]	$\langle x_B\rangle$	$\sigma_{LT'}/\sigma_0$	$\delta_{\rm stat}$	$\delta^{\downarrow}_{\rm sys}$	$\delta^{\uparrow}_{\rm sys}$
0.154	0.09 – 0.20	3.90	2.85	0.36	0.0382	0.0107	0.0281	0.0281
0.242	0.21 – 0.28	4.12	2.78	0.38	0.1012	0.0156	0.0084	0.0041
0.316	0.28 – 0.35	4.30	2.76	0.39	0.0880	0.0200	0.0032	0.0064
0.398	0.35 – 0.45	4.45	2.72	0.40	0.1272	0.0153	0.0108	0.0050
0.574	0.45 – 0.80	4.67	2.66	0.42	0.1356	0.0134	0.0118	0.0054

Table 2: Summary table for setting 2, at central values of Q^2=4.4 GeV^2, x_B=0.4, $\epsilon = 0.715$. Corresponds to Figure 5(b). See caption of Table 1 for more information.

$\langle -t\rangle$ [GeV^2]	$-t$ range [GeV^2]	$\langle Q^2\rangle$ [GeV^2]	$\langle$W$\rangle$ [GeV]	$\langle x_B\rangle$	$\sigma_{LT'}/\sigma_0$	$\delta_{\rm stat}$	$\delta^{\downarrow}_{\rm sys}$	$\delta^{\uparrow}_{\rm sys}$
0.183	0.11 – 0.24	5.07	3.12	0.36	0.0281	0.0253	0.0033	0.0132
0.271	0.24 – 0.30	5.26	3.07	0.38	0.0556	0.0191	0.0036	0.0121
0.347	0.30 – 0.40	5.42	3.04	0.39	0.1324	0.0143	0.0082	0.0052
0.445	0.40 – 0.50	5.56	3.01	0.40	0.1205	0.0200	0.0065	0.0066
0.616	0.50 – 0.80	5.71	2.97	0.42	0.1095	0.0187	0.0046	0.0123

Table 3: Summary table for setting 3, at central values of Q^2=5.5 GeV^2, x_B=0.4, $\epsilon = 0.525$. Corresponds to Figure 5(c). See caption of Table 1 for more information.

$\langle -t\rangle$ [GeV^2]	$-t$ range [GeV^2]	$\langle Q^2\rangle$ [GeV^2]	$\langle$W$\rangle$ [GeV]	$\langle x_B\rangle$	$\sigma_{LT'}/\sigma_0$	$\delta_{\rm stat}$	$\delta^{\downarrow}_{\rm sys}$	$\delta^{\uparrow}_{\rm sys}$
0.026	0.01 – 0.04	1.74	3.04	0.18	0.0310	0.0124	0.0039	0.0039
0.055	0.04 – 0.07	1.87	3.00	0.19	0.0483	0.0071	0.0021	0.0025
0.085	0.07 – 0.10	1.99	2.98	0.20	0.0572	0.0075	0.0021	0.0074
0.115	0.10 - 0.13	2.06	2.96	0.21	0.0803	0.0073	0.0042	0.0034
0.145	0.13 – 0.16	2.11	2.95	0.21	0.0929	0.0075	0.0100	0.0053
0.180	0.16 – 0.20	2.16	2.93	0.22	0.1084	0.0079	0.0104	0.0039
0.244	0.20 – 0.30	2.25	2.91	0.23	0.1055	0.0071	0.0080	0.0037
0.373	0.30 – 0.50	2.38	2.87	0.24	0.1079	0.0103	0.0078	0.0050

Table 4: Summary table for setting 4, at central values of Q^2=2.1 GeV^2, x_B=0.21, $\epsilon = 0.79$. Corresponds to Figure 5(d). See caption of Table 1 for more information.

$\langle -t \rangle$ [GeV^2]	$-t$ range [GeV^2]	$\langle Q^2 \rangle$ [GeV^2]	⟨W⟩ [GeV]	$\langle x_B \rangle$	$\sigma_{LT'}/\sigma_0$	δ_{stat}	$\delta_{\text{sys}}^{\downarrow}$	$\delta_{\text{sys}}^{\uparrow}$
0.046	0.02 – 0.07	2.60	3.24	0.22	0.0324	0.0145	0.0026	0.0039
0.085	0.07 – 0.10	2.77	3.20	0.23	0.0626	0.0100	0.0034	0.0027
0.115	0.10 - 0.13	2.88	3.17	0.24	0.0653	0.0100	0.0034	0.0052
0.145	0.13 – 0.16	2.94	3.16	0.25	0.0822	0.0109	0.0045	0.0055
0.179	0.16 – 0.20	2.99	3.14	0.25	0.1098	0.0092	0.0075	0.0049
0.246	0.20 – 0.30	3.07	3.12	0.26	0.1084	0.0075	0.0061	0.0041
0.379	0.30 – 0.50	3.21	3.09	0.26	0.1123	0.0089	0.0071	0.0057

Table 5: Summary table for setting 5, at central values of Q^2=3.0 GeV^2, x$_B$=0.25 GeV, $\epsilon = 0.67$. Corresponds to Figure 5(e). See caption of Table 1 for more information.

Q^2 Dependence

The following tables provide mean kinematics and final results for each (x$_B$,$-t$) bin used for a Q^2 scan. The CLAS results refer to [1] and CLAS12 refers to [2].

Data set	$\langle -t \rangle$ [GeV^2]	$\langle Q^2 \rangle$ [GeV^2]	$\langle W \rangle$ [GeV]	$\langle x_B \rangle$	$\langle \epsilon \rangle$	$\sigma_{LT'}/\sigma_0$	δ_{stat}	$\delta_{\text{sys}}^{\downarrow}$	$\delta_{\text{sys}}^{\uparrow}$
CLAS	0.108	1.583	2.35	0.254	0.648	0.0893	0.0115	0.0118	0.0118
CLAS12	0.111	1.856	2.53	0.252	0.87	0.0556	0.0078	0.0064	0.0064
CLAS12	0.111	2.784	3.10	0.248	0.661	0.0670	0.0126	0.0048	0.0048
KaonLT	0.115	2.88	3.17	0.244	0.67	0.0653	0.0100	0.0034	0.0052

Table 6: Summary table for Q^2 scan 1 at $x_B = 0.250 \pm 0.006$. Corresponds to Figure 6(a). See caption of Table 1 for more information.

Data set	$\langle -t \rangle$ [GeV^2]	$\langle Q^2 \rangle$ [GeV^2]	$\langle W \rangle$ [GeV]	$\langle x_B \rangle$	$\langle \epsilon \rangle$	$\sigma_{LT'}/\sigma_0$	δ_{stat}	$\delta_{\text{sys}}^{\downarrow}$	$\delta_{\text{sys}}^{\uparrow}$
CLAS12	0.365	2.629	2.18	0.405	0.895	0.1337	0.0119	0.0119	0.0119
KaonLT	0.376	3.02	2.29	0.406	0.885	0.1263	0.0233	0.0115	0.0110
KaonLT	0.347	5.42	3.04	0.394	0.525	0.1324	0.0143	0.0082	0.0052

Table 7: Summary table for Q^2 scan 2 at $x_B = 0.400 \pm 0.006$. Corresponds to Figure 6(b). See caption of Table 1 for more information.

Quantitative Analysis of Models

In this section, we present the χ^2/NDF for each theoretical model for each setting. The data point at the lowest $-t$ for each setting is excluded from this calculation, as it falls below the minimum $-t$ at the mean kinematics where the model is evaluated. The standard formula $\chi^2 = \sum_{i=1}^{n} (y_i - f(t_i))^2 \delta_i^{-2}$ is used, where y_i are the experimental values of $\sigma_{LT'}/\sigma_0$ at t_i, $f(t_i)$ are the model predictions for $\sigma_{LT'}/\sigma_0$ at t_i, and δ_i are the experimental uncertainties at each data point. As the models do not include parameters fixed to data, the NDF is simply the number of data points used in the calculation of χ^2.

It is worth noting that the χ^2/NDF of the VR model may be artificially low due to the exact kinematics of this experiment. The VR model fits much better at lowest $-t$, where most of the data in this experiment is taken, and worse at higher $-t$, where there is only one t-bin. The χ^2/NDF would be much higher if we included higher $-t$ data, for example the CLAS12 data shown in Fig.5(e).

Setting (Q^2 [GeV^2], x$_B$)	1 (3.0, 0.4)	2 (4.4, 0.4)	3 (5.5, 0.4)	4 (2.1, 0.21)	5 (3.0, 0.25)	Average –
YCK1	1.4	1.9	3.0	19.3	8.2	6.8
YCK2	11.1	44.8	11.6	41.3	36.8	29.1
GK1	20.0	17.0	92.5	79.7	232	88.2
GK2	4.2	6.2	17.5	28.8	112	33.7
VR	3.2	13.6	24.7	11.2	14.6	13.5

Table 8: The reduced χ^2 comparing experimental $\sigma_{LT'}/\sigma_0$ to model calculations at each setting. The models are described in the text and exact values of data for each setting are provided above.

Asymmetry Plots

The following figures contain the asymmetry A_{LU} in each $-t$ bin. $\sigma_{LT'}/\sigma_0$ is extracted from A_{LU} according to the equation

$$A_{LU} = \frac{\sqrt{2\epsilon(1-\epsilon)}\frac{\sigma_{LT'}}{\sigma_0}\sin\phi}{1+\sqrt{2\epsilon(1+\epsilon)}\frac{\sigma_{LT}}{\sigma_0}\cos\phi+\epsilon\frac{\sigma_{TT}}{\sigma_0}\cos 2\phi} \tag{1}$$

where $\sigma_0 = \sigma_T + \epsilon\sigma_L$ is the unpolarized cross section, ϵ is the ratio of longitudinal and transverse virtual photon polarization, σ_{LT}, σ_{TT}, $\sigma_{LT'}$ are interference cross sections, and ϕ is the scattering plane angle (Fig. 1). A_{LU} is sometimes approximated as

$$A_{LU} = \sqrt{2\epsilon(1-\epsilon)}\frac{\sigma_{LT'}}{\sigma_0}\sin\phi \tag{2}$$

where the terms σ_{LT}/σ_0 and σ_{TT}/σ_0 are considered to be negligible. In this work, $\sigma_{LT'}/\sigma_0$ is extracted using Eqn. 1, and the value from Eqn. 2 is used to determine a systematic uncertainty.

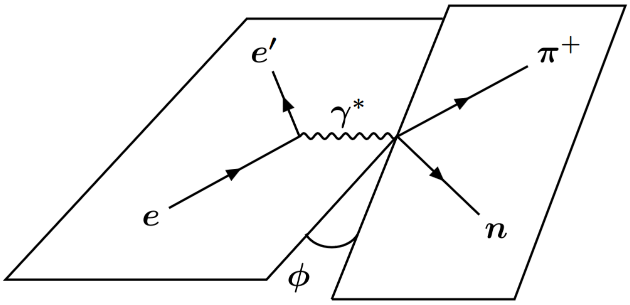

Figure 1: Reaction diagram for $p(e,e'\pi^+)n$. The angle ϕ is defined as the azimuthal angle between the electron scattering plane (defined by e and e') and the hadron reaction plane (defined by π^+ and n).

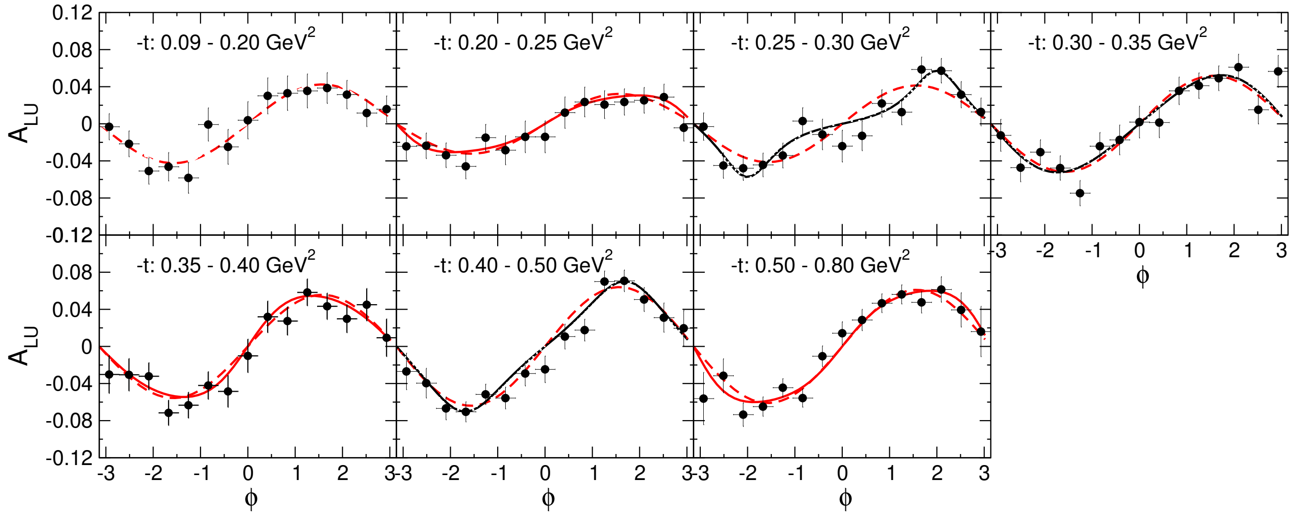

Figure 2: Binned asymmetry for setting 1, at central values of Q^2=3.0, x_B=0.4. The solid line shows the full fit according to Eqn. 1, and the dashed line shows the approximated fit from Eqn. 2. Uncertainties are statistical only.

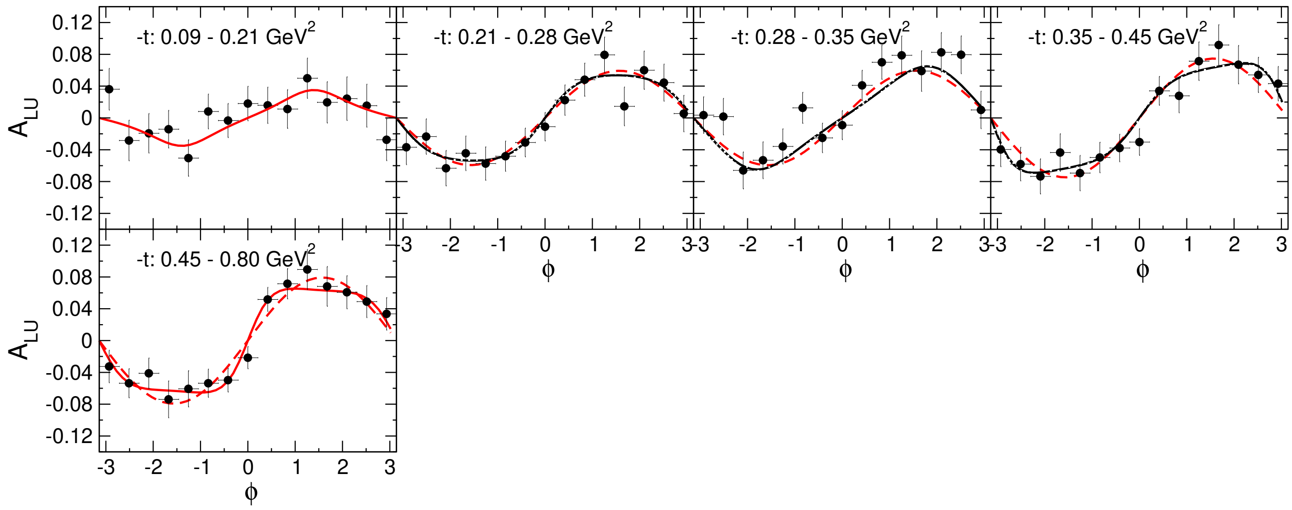

Figure 3: Binned asymmetry for setting 2, at central values of Q^2=4.4, x_B=0.4. The solid line shows the full fit according to Eqn. 1, and the dashed line shows the approximated fit from Eqn. 2. Uncertainties are statistical only.

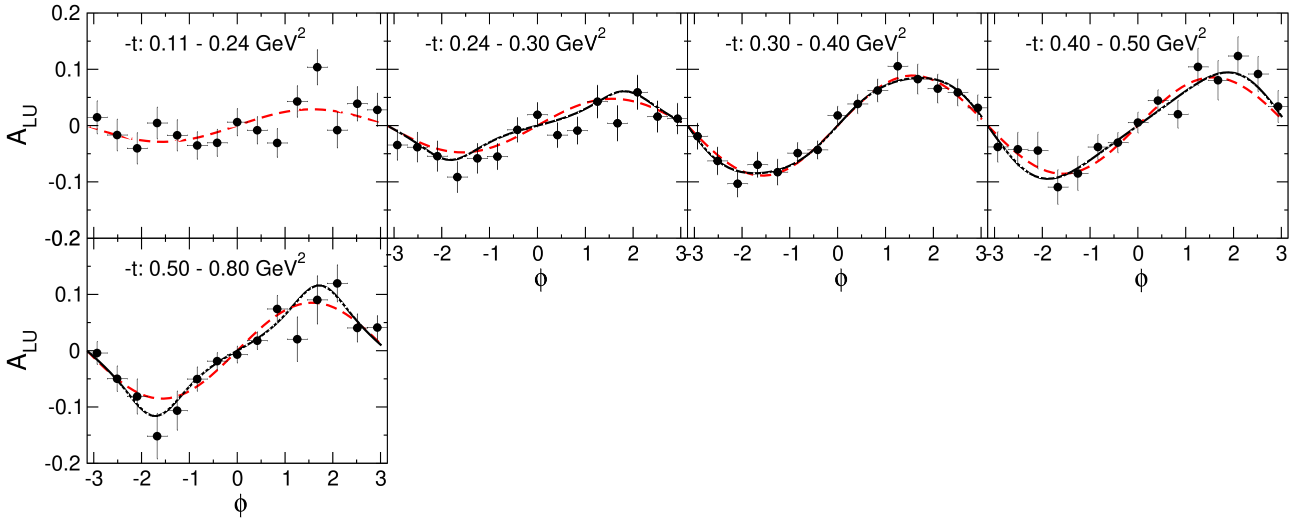

Figure 4: Binned asymmetry for setting 3, at central values of Q^2=5.5, x_B=0.4. The solid line shows the full fit according to Eqn. 1, and the dashed line shows the approximated fit from Eqn. 2. Uncertainties are statistical only.

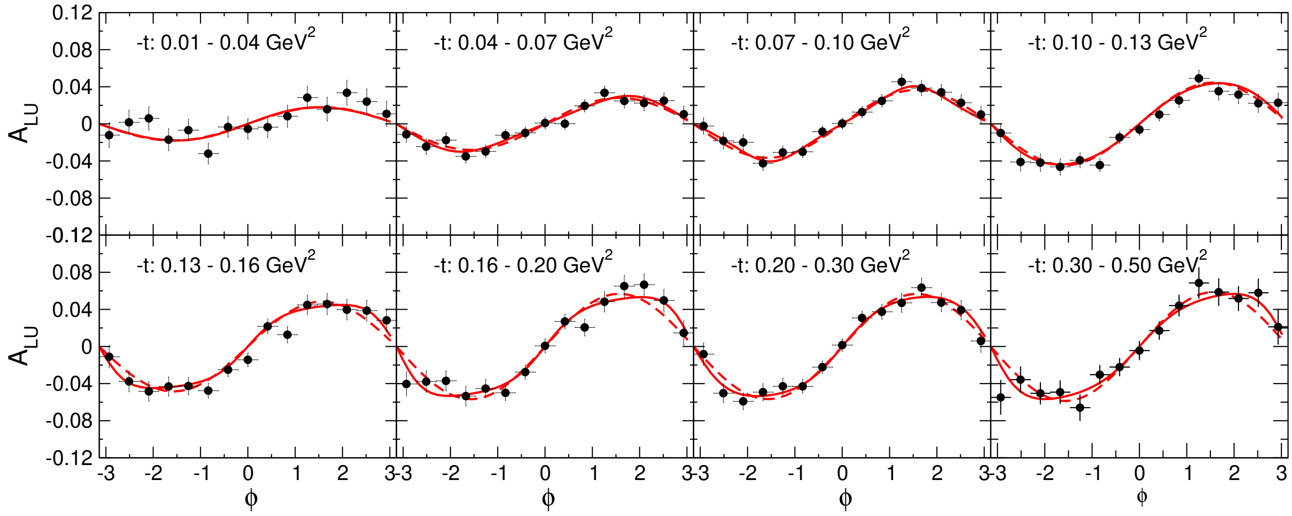

Figure 5: Binned asymmetry for setting 4, at central values of Q^2=2.1, x_B=0.21. The solid line shows the full fit according to Eqn. 1, and the dashed line shows the approximated fit from Eqn. 2. Uncertainties are statistical only.

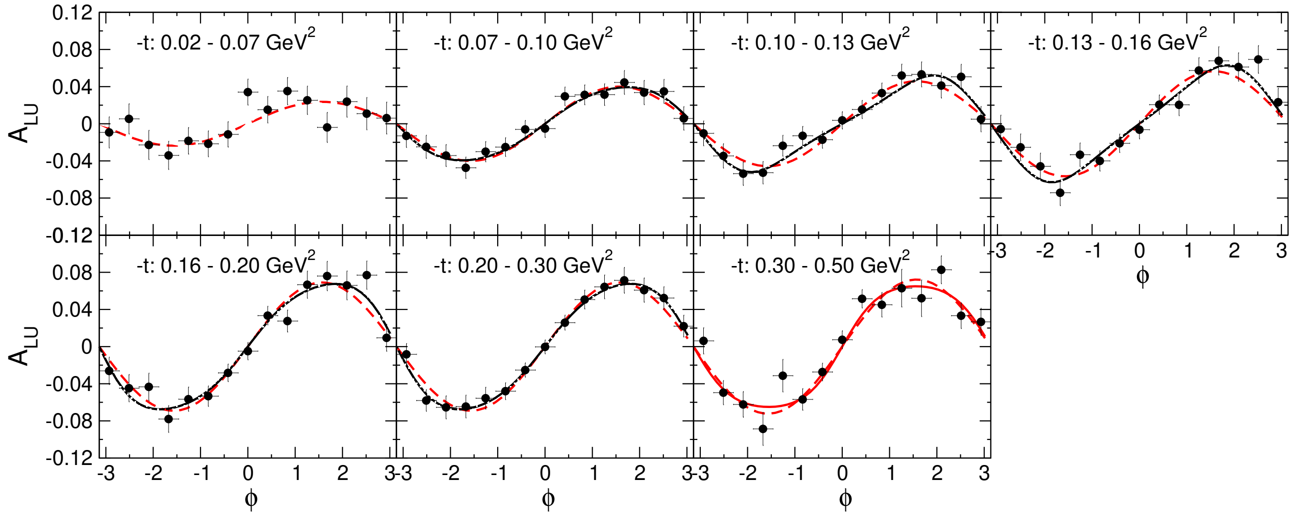

Figure 6: Binned asymmetry for setting 5, at central values of Q^2=3.0, x_B=0.25. The solid line shows the full fit according to Eqn. 1, and the dashed line shows the approximated fit from Eqn. 2. Uncertainties are statistical only.

References

[1] S. Diehl *et al.* (CLAS Collaboration), *Extraction of Beam-Spin Asymmetries from the Hard Exclusive π^+ Channel off Protons in a Wide Range of Kinematics*, Phys. Rev. Lett. **125** 182001 (2020).

[2] S. Diehl *et al.* (CLAS Collaboration), *A multidimensional study of the structure function ratio $\sigma_{LT'}/\sigma_0$ from hard exclusive π^+ electro-production off protons in the GPD regime*, Phys. Lett. B **839** 137761 (2023).